Anomalous brain activation during face and gaze processing in Williams syndrome

D. Mobbs, BSc; A.S. Garrett, PhD; V. Menon, PhD; F.E. Rose, PhD; U. Bellugi, EdD; and A.L. Reiss, MD

Abstract—*Objective:* To investigate the discrete neural systems that underlie relatively preserved face processing skills in Williams syndrome (WS). *Methods:* The authors compared face and eye-gaze direction processing abilities in 11 clinically and genetically diagnosed WS subjects with 11 healthy age- and sex-matched controls, using functional MRI (fMRI). *Results:* Compared to controls, WS subjects showed a strong trend toward being less accurate in determining the direction of gaze and had significantly longer response latencies. Significant increases in activation were observed in the right fusiform gyrus (FuG) and several frontal and temporal regions for the WS group. By comparison, controls showed activation in the bilateral FuG, occipital, and temporal lobes. Between-group analysis showed WS subjects to have more extensive activation in the right inferior, superior, and medial frontal gyri, anterior cingulate, and several subcortical regions encompassing the anterior thalamus and caudate. Conversely, controls had greater activation in the primary and secondary visual cortices. *Conclusion:* The observed patterns of activation in WS subjects suggest a preservation of neural functioning within frontal and temporal regions, presumably resulting from task difficulty or compensatory mechanisms. Persons with WS may possess impairments in visual cortical regions, possibly disrupting global-coherence and visuospatial aspects of face and gaze processing.

NEUROLOGY 2004;62:2070–2076

Williams syndrome (WS) is a neurodevelopmental condition characterized by a 1.5 Mb deletion on chromosome 7 (band 7q11.23).[1-3] This deletion results in a constellation of strengths and weaknesses in higher-cognitive domains, including gross impairments in global-coherence, visual-spatial, math, and problem solving skills.[4-7] By contrast, despite mild to moderate mental retardation, affected individuals demonstrate relatively proficient expressive language skills, a vigorous social drive, and distinct musical interests.[5,8,9] Thus the presence of a predictable dissociation in cognition presents an opportunity to explore discrete genotype-phenotype correlations.

An additional neurocognitive hallmark of WS is a relative strength in the recognition and discrimination of faces. Studies utilizing several standardized face processing tests have illustrated WS subjects' characteristic ability to consistently outperform IQ matched subjects, and even perform near the level of healthy controls.[5,8,10-12] Additionally, affected individuals are unusually drawn to faces, seek direct eye gaze,[13] and rate unfamiliar faces as being more approachable.[8,14] As a result, WS differs from some neurodevelopmental syndromes, including autism, where conspicuous impairments in face processing are documented.[15-17]

Here, we use fMRI to elucidate the proficient face and eye-gaze processing abilities in WS. Our use of face processing in conjunction with eye-gaze was driven by an attempt to understand the cognitive and socio-emotive aspects of face processing in WS. Thus, in order to optimally activate the network of regions involved in face perception, increase social salience, and minimize the confound of emotion processing, we presented faces having neutral expression at both forward and angled orientations and with both direct and averted gaze.

Because they seek out faces and gaze, we hypothesized that individuals with WS would exhibit relatively normal levels of activation within face processing pathways, including the fusiform gyrus (FuG), superior temporal sulcus (STS), and amygdala. We further hypothesized that regions associated with social attention, including the medial frontal gyrus and the anterior cingulate cortex (ACC), would be employed to a greater extent in WS subjects.

Materials and methods. *Subjects.* WS subjects were recruited as part of an ongoing program, which includes event-related potential (ERP), behavioral, molecular genetics, histologic, and volumetric MRI studies.[3,5,8,18-20] We recruited 18 individuals with a diagnosis of WS (10 female) for the fMRI aspect of this project. Seven of these subjects were later excluded from the data analyses due to poor task performance (i.e., no response), head

From the Department of Psychiatry & Behavioral Sciences (D. Mobbs and Drs. Garrett, Menon, and Reiss), Program in Neuroscience (Drs. Menon and Reiss), Stanford Brain Research Institute (Drs. Menon and Reiss), Stanford University School of Medicine; and the Laboratory for Cognitive Neuroscience (Drs. Rose and Bellugi), The Salk Institute for Biological Studies, La Jolla, CA.

Supported by the following grants from the National Institutes of Health: MH01142, MH50047, HD31715, HD33113, and HD40761.

Received July 17, 2003. Accepted in final form February 2, 2004.

Address correspondence and reprint requests to Dr. Allan L. Reiss, Department of Psychiatry and Behavioral Sciences, Stanford University School of Medicine, 401 Quarry Road, Stanford, CA 94305–5719; e-mail: reiss@stanford.edu

 Copyright © 2004 by AAN Enterprises, Inc.

Copyright © by AAN Enterprises, Inc. Unauthorized reproduction of this article is prohibited.

movement, or problems with image acquisition. The remaining 11 subjects consisted of 8 female and 3 male subjects, mean age ± SD 30.6 ± 11.7 years. All genetic diagnoses were confirmed using florescent in situ hybridization (FISH) probes for elastin (ELN), a gene consistently found in the microdeletion associated with WS.[2,3] In addition, all participants exhibited the medical and clinical features of the WS phenotype, including cognitive, behavioral, and physical profiles.[5]

Controls were 11 healthy volunteers, 9 female and 2 male (mean age = 33.9 ± 10.7 years). Control subjects were screened for a history of psychiatric or neurologic problems using the Symptom Checklist-90-R (SCL-90-R).[21] All subjects had SCL-90-R scores that fell within one SD of a normative sample. Cognitive functioning was assessed by using the Wechsler Intelligence Scale for Children, Revised (third edition; WISC-III) for those under 16 years of age, and the Wechsler Adult Intelligence Scale, third edition (WAIS-III) for ages 16 and up. Both the WAIS-III and WISC-III assessed Verbal IQ (VIQ), Performance IQ (PIQ), and Full-Scale IQ (FSIQ). The average FSIQ score for the WS group was 66.4 ± 11.5 (mean ± SD). VIQ scores (72.0 ± 11.9) were generally higher than PIQ scores (64.0 ± 11.5). All controls were within two SD of the normal range of intelligence (FSIQ = 117 ± 10.0; VIQ = 108.6 ± 16.6; PIQ = 117.0 ± 10.0).

We avoided controlling for IQ between WS and control subjects for several reasons: 1) because of their peaks and valleys in cognition,[5] conventional intelligence scales are not a valid indicator of specific skills as they measure aggregated cognitive function, including several domains that are known to be disproportionately impaired in WS.[22] On the other hand, we chose a cognitive area of strength for subjects with WS for this initial fMRI study; 2) the use of IQ matched subjects, for example developmentally delayed, is problematic given that retardation may involve diverse and unspecified forms of CNS pathology. Therefore idiopathic mentally retarded control subjects do not necessarily constitute a healthy developing comparison for WS populations; and 3) using a population of WS affected subjects with high IQs, which is common in those with partial deletions, may also be unrepresentative of typical WS populations.

All WS and control subjects were right-handed, native English speakers, and provided written informed consent before participation. All experimental procedures complied with the standards of the human subjects committee at Stanford University School of Medicine.

Experimental stimuli. A total of 105 color stimuli were presented in a blocked fMRI paradigm with 30-second epochs corresponding to each of the two task conditions (figure 1). Sixty of the images were static color pictures of faces of college-aged models and 45 were isoluminant scrambled images of these pictures. Isoluminant scrambled images were split into 256 parts similar to those used in previous studies of face processing.[23] All models displayed a neutral facial expression. Four different categories of face and gaze orientation were used, consisting of face and gaze directed forward; face forward with gaze averted 45°; face angled 45° with gaze directed forward; and face angled 45° with gaze averted 45°. The number of pictures in which the face and gaze angled to the right was balanced with the number of pictures angled to the left. To avoid repetition effects, no picture was presented twice. Stimuli were presented using PsyScope software[24] in conjunction with a custom-built projector (Resonance Technology, Los Angeles, CA), which projected the stimuli onto a screen attached to the head-coil.

Experimental paradigm. The task consisted of rest, experimental (E; faces), and control (C; scrambled blocks) epochs in the following order: Rest-E-C-E-C-E-C-E-Rest (see figure 1). Thus there were two rest epochs, four experimental epochs, and three control epochs in the task. Each rest epoch was 30 seconds long during which subjects passively viewed a blank screen. Each control and experimental epoch consisted of 15 stimuli presented for 1,750 msec each, with a 250 msec interstimulus interval (ISI). Each epoch lasted 30 seconds. In the experimental epoch, the four conditions were randomly alternated. In order to maintain their attention to the stimuli, subjects were asked to indicate if the gaze was directed at or away from them by pressing the left or right button (with the first and second fingers of the right hand). In the control epoch, subjects were instructed to alternately press the two buttons. Subject response time (RT) was recorded for 2 seconds, from the beginning of each presentation until the end of the

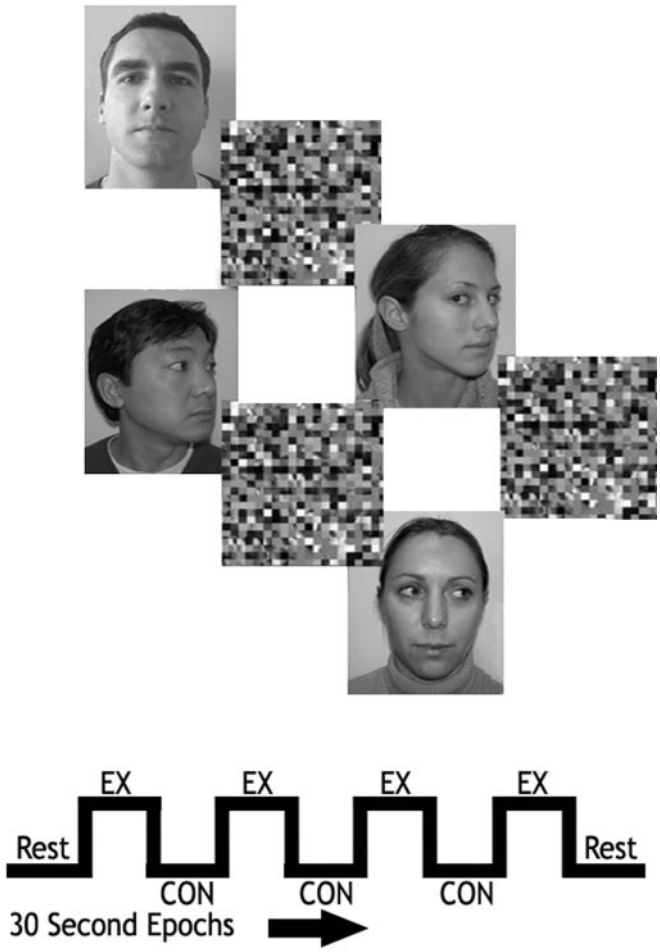

Figure 1. Blocked design illustrating examples of the alternating angled and forward positioned faces/eye gaze (EX = experimental condition) and isoluminant scrambled blocks (CON = control condition). During the 4 minute, 36 seconds scan, subjects were presented with 60 nonrepeating face stimuli across four epochs, and 45 isoluminant scrambled images across three epochs. Each epoch lasted 30 seconds.

250 msec ISI. Correct and incorrect responses and reaction times were recorded if they occurred between 150 and 2,000 msec after the stimulus. Prior to the scan, research staff worked with each subject to insure that they were capable of attending to and performing the task in the scanner.

Image acquisition. Structural and functional images were acquired on a 1.5-T GE Signa scanner (General Electric Medical Systems, Milwaukee, WI) with Echospeed gradients using a custom-built, whole-head coil.[25] Eighteen axial slices (6 mm thick, 1 mm skip) parallel to the anterior and posterior commissures, covering the whole brain, were imaged with a temporal resolution of 2 seconds using a T2*-weighted, gradient echo, spiral pulse sequence (time to repetition [TR] = 2,000 msec, time to echo [TE] = 40 msec, flip angle = 89°, and 1 interleave).[26] The field of view (FOV) was 240 mm, and the effective in-plane spatial resolution was 4.35 mm. To aid in localization of functional activation, a high-resolution, T1-weighted, spoiled gradient-recalled, three-dimensional MRI sequence with the following parameters was used: TR = 35 msec; TE = 6 msec; flip angle = 45°; 24 cm FOV; 124 slices in coronal plane; 256 × 192 matrix; acquired resolution = 1.5 × 0.9 × 1.2 mm.

Image analysis. Images were reconstructed by inverse Fourier transform for each of the 135 time points into 64 × 64 × 18 image matrices (voxel size: 3.75 × 3.75 × 7 mm). Then, fMRI data were analyzed using SPM99 (http://www.fil.ion.ucl.ac.uk/spm).

Copyright © by AAN Enterprises, Inc. Unauthorized reproduction of this article is prohibited.

Images were corrected for movement using least square minimization without higher-order corrections for spin history, and normalized to stereotaxic Talairach coordinates.[27] Images were then resampled every 2 millimeters using sinc interpolation and smoothed with a 4 millimeter Gaussian kernel to decrease spatial noise. The general linear model and the theory of Gaussian random fields implemented in SPM99 were used to complete statistical analyses of fMRI data.[28] For each subject, activation was calculated at each voxel and corrected for temporal autocorrelation. Confounding effects of fluctuations in global mean were removed by proportional scaling where each voxel was scaled by the global mean at each time-point. Low frequency noise was removed by applying a high pass filter (0.5 cycles/minute) to the fMRI time series at each voxel. A temporal smoothing function (Gaussian kernel corresponding to dispersion of 8 seconds) was applied to the fMRI time-series to enhance the temporal signal to noise ratio.

For each subject, a *t*-score image was generated for each contrast of interest (i.e., faces minus scrambled faces). Group analyses used a random-effects model incorporating a two-stage hierarchical procedure, thus providing a stronger generalization to the population.[29] In the first step, contrast images for each subject were generated as described above. In the second step, contrast images were combined into a group image using a general linear model. Significant clusters of activation were determined using the joint expected probability of height ($Z > 1.96$, $p < 0.05$) and extent ($p < 0.05$) of Z scores,[30] yielding a cluster-wise level of $p = 0.05$, after correction for multiple comparisons. Activation foci were superimposed on high-resolution T1-weighted images and localized with reference to the stereotaxic atlas of Talairach and Tournoux.[27] Because the contrasts examined in this study were chosen a priori (faces vs scrambled faces), activations from other contrasts are not reported here.

Region of interest analysis. To substantiate whole-brain activation, anatomically defined regions of interest (ROI) were circumscribed for each group on a T1-weighted spatially normalized, high-resolution structural image. The choice of ROIs was based on previous neuroanatomic, neurophysiologic, and neuropsychological findings from our group.[18-20,31] These data indicated that anterior-ventral cerebral regions were more anatomically and functionally intact than posterior-dorsal areas in WS. ROIs were also based on previous findings from neuroimaging studies of face and eye-gaze.[22] Accordingly, anatomic ROIs were generated for the bilateral visual cortex, fusiform gyrus, superior temporal sulcus, and amygdala. The anatomic boundaries of all regions were drawn on contiguous, high-resolution coronal images using BrainImage software.[32] The number of activated voxels (defined as $Z > 1.67$) in each ROI was compared between groups using the nonparametric Mann-Whitney *U* test. A two-tailed threshold of $p < 0.05$ was used in these analyses.

Fusiform gyrus. The FuG begins at the coronal slice containing the largest cross-section of the anterior commissure. The lateral border of the FuG was defined by the lateral occipito-temporal sulcus. The inferior border was delineated by following the surface of the cortical matter. The medial border of the FuG was defined by the collateral sulcus. The posterior border of the FuG was determined in two steps: First, the sagittal plane tangent to the lateral border of the amygdala was identified. Second, the previously identified sagittal slice, the coronal plane crossing at the level of the posterior transverse collateral sulcus delineated the most posterior slice of the FuG.

Superior temporal sulcus. The STS was drawn from its origin in the anterior temporal pole. The first slice was drawn on the head of the putamen at the slice with the thickest anterior commissure. The most posterior slice was defined as the slice where the pillar of the fornix was visible. On each coronal slice, the sulcus ROI was defined as the gray matter between the peak of the STS and the peak of the interior temporal sulcus, including all gray matter in the STS.

Amygdalar nuclei. The anterior slice was identified in the coronal plane at the level where the white matter of the anterior commissure first crosses the midline. The posterior slices corresponded to the last coronal slice where the hippocampus is identifiable and the structure was measured until it was no longer visible. The inferior border of the amygdala was marked, rostal-caudal, by the white matter tract of the temporal pole, temporal horn of the lateral ventricles, and hippocampus. The medial superior border was defined by the entorhinal sulcus. The lateral border of the amygdala was marked by white matter.

Visual cortex. The visual cortex ROI encompassed Brodmann areas (BA) 17, 18, and 19, including the cuneus and lingual gyrus. It included the last slice with visible corpus callosum, proceeding posterior though the lingual gyrus to the parieto-occipital fissure. Here, we included the lateral portions of the brain (inferior, middle, and lateral occipital gyri), but excluded the angular and superior parietal gyri.

Results. *Behavioral analysis.* Both WS (73.6% ± 16.8%) and controls (87.1% ± 14.4%) performed the task above chance. Independent-samples *t*-tests (two-tailed) were conducted revealing a statistical trend, but no difference in accuracy when WS and controls were compared ($t^{20} = -2.0$, $p < 0.057$). Analysis of RT (mean RT ± SD in milliseconds), however, showed WS subjects (1,030.8 ± 103.3 msec) to be slower than controls (803.1 ± 61.9 msec) ($t^{20} = 6.3$, $p < 0.0001$) in determining the direction of gaze. In the control condition, no significant differences for accuracy or RT were found between the groups.

Brain activation. The primary voxel-based analysis compared neural activation during face/gaze stimuli to activation during blocks of scrambled stimuli (tables 1 and 2; figure 2, A through C). Within-group analysis of WS subjects revealed activation of several structures, predominantly anterior in location. The largest cluster of activation included the right thalamus/pulvinar, right superior frontal gyrus (SFG; BA 8) extending to the dorsal ACC (BA 32), and adjoining the MFd, and pre-supplementary motor area (SMA; BA 6). A second cluster was observed in the right inferior frontal gyrus (IFG; BA 44) extending to the middle frontal gyrus (MFG; BA 9). WS subjects also showed activation in the right FuG, traversing caudally to the inferior occipital gyrus (IOG) and cerebellum, and rostrally to the parahippocampal gyrus (PHG) and hippocampus (HIPP). A fourth cluster was observed in the left lentiform nucleus, extending to left thalamus and bilateral caudate and putamen (see table 1, figure 2B). In comparison, controls showed relatively greater activation for the faces compared to the scrambled condition in predominantly posterior regions. The peak of this large cluster was in the right middle occipital gyrus (MOG; BA 19) (see figure 2A). This region of activation proceeded to several additional structures including the left HIPP, and several bilateral regions including the PHG, lingual gyri, middle and inferior temporal gyri (MTG/ITG) (BA 39), FuG, and precuneus (Pcu) (BA 31) (see table 2).

Between-group analyses revealed striking differences in the topography of relative brain activation (see figure 2C). Compared to controls, the WS group showed greater activation within right prefrontal (superior, middle, and inferior frontal gyri), ACC, thalamic, striatal and temporal (hippocampus, middle temporal gyrus) areas. However, the WS group exhibited significantly less activation than controls in primary and secondary visual cortices (BA 17, 18, 19) and the right Pcu (BA 31).

Region of interest results. A Mann-Whitney *U* test comparing percent voxel activation during face processing between groups showed controls to have significantly greater percentage of voxels activated in the visual cortex ($Z = -2.2$, $p = 0.028$). However, there were no significant between-group differences in the amygdala: left ($Z = -1.216$, $p = 0.224$) and right ($Z = -0.952$, $p = 0.341$); FuG: left ($Z = -0.361$, $p = 0.718$) and right ($Z = -1.346$, $p = 0.193$); and STS: left ($Z = -0.558$, $p = 0.577$) and right ($Z = -0.821$, $p = 0.412$).

Copyright © by AAN Enterprises, Inc. Unauthorized reproduction of this article is prohibited.

Table 1 *Brain areas in which face perception stimuli-related blood oxygenation level dependent activation was significant over and above scrambled blocks (p < 0.05 corrected)*

Regions	Brodmann area	*p* Value	Cluster size, voxel	t-Score	Talairach coordinates X	Y	Z
Williams syndrome group (n = 11)							
Right thalamus,* pulvinar	—	<0.001	1,440	3.96	10	−8	2
Left lentiform nucleus,* left thalamus, bilateral putamen, and caudate	—	<0.012	769	3.60	−24	−18	4
Right SFG,* right ACC, right MFd, right pre-SMA	8/32	<0.006	853	4.07	4	16	48
Right IFG,* MFG, left globus pallidus, lateral ventrical, HIPP, and PHG	44/9	<0.001	1,245	4.42	52	12	22
Right FuG,* IOG, cerebellum, HIPP, and PHG	37	<0.001	2,311	4.59	50	−66	16
Control group (n = 11)							
Right MOG,* left HIPP, right Pcu and bilateral PHG, FuG, LG, cerebellum, and MTG/ITG	19/39	<0.001	13,744	5.58	46	−76	−6

Only clusters with a significance value of $p < 0.05$ corrected for whole brain are reported. Stereotaxic coordinates as in Talairach and Tournoux (1988) atlas space.

* Peak activation.

SFG = superior frontal gyrus; ACC = anterior cingulate cortex; MFd = medial frontal gyrus; SMA = supplementary motor area; IFG = inferior frontal gyrus; MFG = middle frontal gyrus; HIPP = hippocampus; PHG = parahippocampal gyrus; FuG = fusiform gyrus; IOG = inferior occipital gyrus; MOG = middle occipital gyrus; Pcu = precuneus; LG = lingual gyrus; MTG = middle temporal gyrus; ITG = inferior temporal gyrus.

Discussion. Behaviorally, WS subjects had longer response latencies and were somewhat less accurate than controls, suggesting that they found the task more difficult than controls. Increased activation was observed in the right FuG and several frontal and temporal regions for WS subjects. Unaffected controls showed increased activation in expected regions including the FuG, occipital, and temporal lobe bilaterally. Between-group analysis, however, revealed striking differences with WS subjects possessing greater activation in the right superior, middle, medial, and inferior frontal gyri, right medial temporal lobe, and bilateral ACC and thalamus. This sharply contrasted with the control group, who showed greater activation in posterior regions bilaterally, including the primary and secondary visual cortices (BA 17, 18, 19, 31). Together, these data act as a potential link among previous behavioral, histologic, ERP, and MRI studies of this disorder.[18-20,31,33]

The relative decreases in visual cortical activation as shown by whole-brain and ROI analysis in WS subjects converge with previous MRI studies from our group showing excessive gray matter loss in the occipital lobe in WS subjects.[20] Similarly, a postmor-

Table 2 *Voxel coordinates in Talairach space and associated z-scores showing the blood oxygenation level dependent differences between controls minus Williams Syndrome (WS) and vice versa (p < 0.05 corrected)*

Regions	Brodmann area	*p* Value	Cluster size, voxel	t-Score	Talairach coordinates X	Y	Z
WS minus controls							
Right SFG,* MFd, ACC, pre-SMA, thalamus, and bilateral putamen	8/9/32	<0.001	3,218	4.23	4	16	48
Left globus pallidus,* lateral ventrical, posterior HIPP, and PHG	—	<0.001	1,459	3.42	−22	−16	2
Right IFG,* MTG	21/45	<0.001	826	3.05	56	22	6
Controls minus WS							
Right precuneus,* right cuneus, left lingual gyrus, primary visual cortex	17/18/19/31	<0.001	2,280	4.46	14	−70	22

Only clusters with a significance value of $p < 0.05$ corrected for whole brain are reported.

* Peak activation.

SFG = superior frontal gyrus; MFd = medial frontal gyrus; ACC = anterior cingulate cortex; SMA = supplementary motor area; HIPP = hippocampus; PHG = parahippocampal gyrus; IFG = inferior frontal gyrus; MTG = middle temporal gyrus.

Copyright © by AAN Enterprises, Inc. Unauthorized reproduction of this article is prohibited.

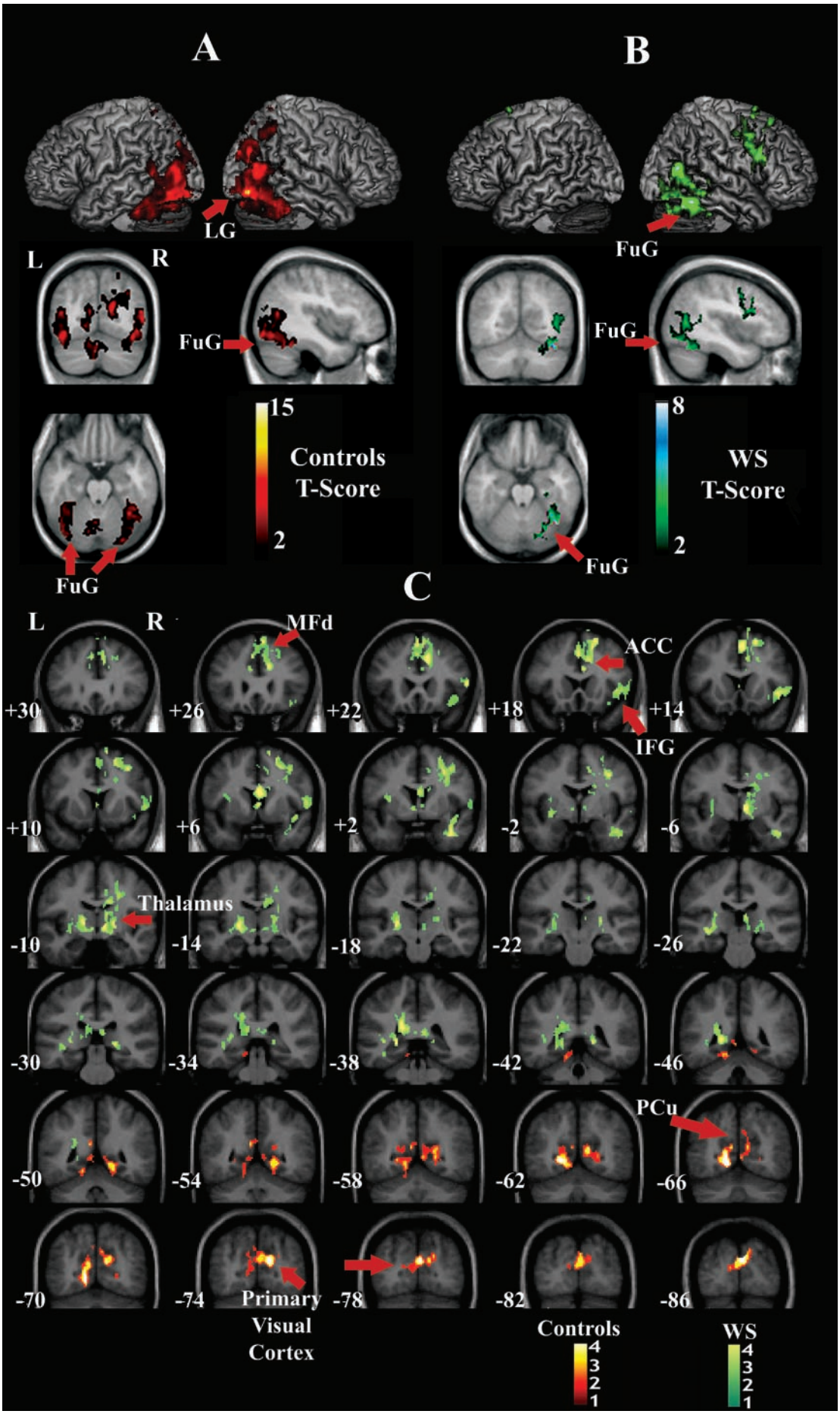

Figure 2. Within group t-maps for both typically developing controls (A) and Williams syndrome (WS) affected individuals (B) showing significant regions of activation. Activation was superimposed on normalized brains of respective groups. Note the preserved right FuG activation in WS subjects; (C) composite dual montage showing significant between group differences. Clusters were color coded with green denoting WS affected subjects' activation, and red, yellow, and orange denoting comparison controls (for abbreviations, see table 1). Brain activation was superimposed on the average T1-weighted normalized image of all participants (n = 22).

Copyright © by AAN Enterprises, Inc. Unauthorized reproduction of this article is prohibited.

tem histologic study showed significantly smaller and more densely packed cells in the peripheral visual cortex of WS subjects.[31] These anomalies may, in part, underlie the higher incidence of visual-perceptual problems in WS, including reduced stereopsis and visual acuity.[34] Moreover, these studies suggest that anomalies in neuronal morphology and synaptic connectivity in visual regions may result in diminished BOLD signal as measured by fMRI.

The finding of heightened frontal activation in the right prefrontal cortex of WS subjects is compelling in light of several recent studies utilizing different research modalities. Quantitative postmortem studies of gross neuroanatomy in WS subjects have revealed a pattern of relative sparing of frontal cortical volume, but disproportional reductions in the parietal-occipital cortex.[18,35] Several MRI studies have shown relative volumetric integrity of the frontal lobe.[20] The exact role of frontal lobe regions in face processing, however, remains unclear. One PET study showed that the right PFC is recruited when the visual clarity of faces is degraded, suggesting that the PFC is needed when face perception becomes more visually demanding.[36]

Increased frontal activation during face and gaze processing in the WS also encompassed the MFd extending to the dorsal portions of the ACC, a region known to have strong connections to the limbic system. The ACC activation is compelling as the abnormal social behavior observed in WS may reflect ACC deficits in "on-off responses" to social stimuli[18] and possibly emotion regulation.[37] Others have suggested that larger N200 peak amplitude in the vicinity of the ACC, as measured by ERP, reflects WS heightened attention to facial stimuli.[19] Thus, the heightened MFd and ACC activation observed in WS subjects may underpin their overtly gregarious, empathetic behavior, and perhaps their partially preserved theory of mind.[38,39] However, it is important to note that this region also is recruited when cognitively taxing tasks are performed. Therefore, frontal overactivation may result from compensatory mechanism related to task demands.

Consistent with our hypothesis, both WS subjects and controls showed significant activation in the right FuG. Functional brain imaging studies conducted on typically developing individuals, in addition to electrophysiologic, and primate homologues, have reliably implicated the FuG in face processing.[40-43,50-53] However, the variables that modulate FuG activity have been vigorously debated. One theory is that the FuG is concerned with perceptual expertise, rather than face perception,[44] since activation of the FuG increases with expertise for recognizing novel objects.[45] Moreover, FuG activation increases with attention,[46] and social interest.[47] Recently, the right FuG has been implicated in abstract semantic knowledge associated with faces and retrieved for social computations.[48] These theories are compelling in light of the diminished or absent FuG activation in autistic subjects[15,16] who often show abnormal eye gaze. Therefore, the increased social interest in WS may account for the normal levels of FuG activation in this population.

It is important to consider whether brain activation in WS results from the use of aberrant, yet effective, processing strategies. Although recently disputed,[53] neuropsychological studies have suggested that WS individuals utilize a feature-based strategy when processing face stimuli. Additionally, when made to use a global-configural strategy,[49] a strategy observed in typically developing individuals, they perform significantly below their usual standards.[54] Prior neuroimaging studies suggest that global-coherence tasks activate the right occipital lobe,[55] including early retinotopically mapped regions,[56] regions activated only in our control group. Although the data presented here do not permit definitive conclusions regarding strategic differences, our results suggest, and echo previous claims,[54] that WS subjects undergo an abnormal developmental course in face processing and may compensate for early visual-perceptual deficits by utilizing more anterior regions to accomplish a feature-based approach to face processing. It is important to note, however, that to verify this, future studies should aim to disentangle task demands from anomalous frontal activation.

Although we sought to activate those regions involved in both cognitive and socio-emotive aspects of face processing in WS, due to the limitations imposed by a blocked-design, we were unable to tease apart face processing from gaze orientation. To overcome these limitations, future studies should consider using an event-related design. Future research should also aim to determine the effect of group differences in strategy or attention on cortical activation in WS population, for example, by tracking eye movements. This would help clarify the question of whether visual attention results in more visual cortical activation.

Notwithstanding these limitations, the present investigation presents preliminary results characterizing the neural correlates of relatively preserved face-processing skills in WS. Whole-brain and ROI results strongly converge with prior morphometric, histologic, and ERP studies demonstrating topographic differences along the anterior-posterior neural axis in WS. Further studies are needed, however, to elucidate and unravel the discrete nexus between molecular genetics and the enigmatic neurocognitive phenotype observed in WS.

Acknowledgment

The authors thank Dr. Julie Korenberg, Asya Karchemskiy, J. Eric Schmitt, Dr. Amy Lightbody, Cindy Johnston, and Katie McKenzie for help in data acquisition and analysis, and the volunteers for their participation in this study.

References

1. Morris CA, Demsey SA, Leonard CO, et al. Natural history of Williams syndrome: physical characteristics. J Pediatr 1988;113:318–326.
2. Ewart AK, Morris CA, Atkinson D, et al. Hemizygosity at the elastin locus in a developmental disorder, Williams syndrome. Nat Genet 1993; 5:11–16.

Copyright © by AAN Enterprises, Inc. Unauthorized reproduction of this article is prohibited.

3. Korenberg JR, Chen XN, Hirota H, et al. VI. Genome structure and cognitive map of Williams syndrome. J Cogn Neurosci 2000;12(suppl 1):89–107.
4. Bihrle AM, Bellugi U, Delis D, et al. Seeing either the forest or the trees: dissociation in visuospatial processing. Brain Cogn 1989;11:37–49.
5. Bellugi U, Lichtenberger L, Jones W, et al. I. The neurocognitive profile of Williams syndrome: a complex pattern of strengths and weaknesses. J Cogn Neurosci 2000;12(suppl 1):7–29.
6. Pani JR, Mervis CB, Robinson BF. Global spatial organization by individuals with Williams syndrome. Psychol Sci 1999;10:453–458.
7. Mervis CB, Robinson BF, Pani JR. Visuospatial construction. Am J Hum Genet 1999;65:1222–1229.
8. Jones W, Bellugi U, Lai Z, et al. II. Hypersociability in Williams syndrome. J Cogn Neurosci 2000;12(suppl 1):30–46.
9. Levitin DJ. Bellugi U. Musical abilities in individuals with Williams syndrome. Music Perception 1998;15:357–389.
10. Udwin O, Yule W. A cognitive and behavioural phenotype in Williams syndrome. J Clin Exp Neuropsychol 1991;13:232–244.
11. Rossen ML, Jones W, Wang PP, et al. Face processing: remarkable sparing in Williams syndrome. Special issue. Genet Couns 1995;6:138–140.
12. Paul BM, Stiles J, Passarotti A, et al. Face and place processing in Williams syndrome: evidence for a dorsal-ventral dissociation. Neuroreport 2002;13:1115–1119.
13. Mervis C, Morris CA, Klein-Tasman BP, et al. Attentional characteristics of infants and toddlers with Williams syndrome during triadic interactions. Dev Neuropsychol 2003;23:243 – 268.
14. Bellugi U, Adolphs R, Cassady C, et al. Towards the neural basis for hypersociability in a genetic syndrome. Neuroreport 1999;10:1653–1657.
15. Pierce K, Muller RA, Ambrose J, et al. Face processing occurs outside the fusiform 'face area' in autism: evidence from functional MRI. Brain 2001;124(Pt 10):2059–2073.
16. Schultz RT, Gauthier I, Klin A, et al. Abnormal ventral temporal cortical activity during face discrimination among individuals with autism and Asperger syndrome. Arch Gen Psychiatry 2000;57:331–340.
17. Elgar K, Campbell R. Annotation: the cognitive neuroscience of face recognition: implications for developmental disorders. J Child Psychol Psychiatry 2001;42:705–717.
18. Galaburda AM, Bellugi UV. Multi-level analysis of cortical neuroanatomy in Williams syndrome. J Cogn Neurosci 2000;12(suppl 1):74–88.
19. Mills DL, Alvarez TD, St George M, et al. III. Electrophysiological studies of face processing in Williams syndrome. J Cogn Neurosci 2000; 12(suppl 1):47–64.
20. Reiss AL, Eliez S, Schmitt JE, et al. IV. Neuroanatomy of Williams syndrome: a high-resolution MRI study. J Cogn Neurosci 2000;12(suppl 1):65–73.
21. Derogatis LR. SCL-90: administration, scoring, and procedures manual. Baltimore: Johns Hopkins University, Clinical Psychometrics Research Unit, 1977.
22. Harris JC. Developmental neuropsychiatry: assessment, diagnosis, and treatment of developmental disorders. Volume II. New York: Oxford University Press, 1995.
23. Hoffman EA, Haxby JV. Distinct representations of eye gaze and identity in the distributed human neural system for face perception. Nat Neurosci 2000;3:80–84.
24. Cohan JD, MacWhinney B, Flatt M, et al. Psyscope: an interactive graphic system for designing and controlling experiments in the psychology laboratory using Macintosh computers. Behavior Research Methods, Instruments & Computers 1993;25:257–271.
25. Hayes CMC. Improved brain coil for fMRI and high resolution imaging. In: Proceedings of the Fourth Annual Meeting of the International Society for Magnetic Resonance in Medicine; Berkeley, CA; 1996;1414.
26. Glover GH, Lai S. Self-navigated spiral fMRI: interleaved versus single-shot. Magn Reson Med 1998;39:361–368.
27. Talairach J, Tournoux P. Coplanar stereotaxic atlas of the human brain. New York: Thieme Medical Publishers, 1988.
28. Friston K, Holmes A, Worsley K, et al. Statistical parametric maps in functional imaging: a general linear approach. Hum Brain Mapp 1995; 2:89–210.
29. Holmes AP, Friston KJ. Generalisability, random effects & population inference. Neuroimage 1998;7:S754.
30. Poline JB, Worsley KJ, Evans AC, et al. Combining spatial extent and peak intensity to test for activations in functional imaging. Neuroimage 1997;5:83–96.
31. Galaburda AM, Holinger DP, Bellugi U, et al. Williams syndrome: neuronal size and neuronal-packing density in primary visual cortex. Arch Neurol 2002;59:1461–1467.
32. Reiss AL. BrainImage. 5. X ed. Stanford, CA: Stanford University.
33. Jernigan TL, Bellugi U, Sowell E, et al. Cerebral morphologic distinctions between Williams and Down syndromes. Arch Neurol 1993;50: 186–191.
34. Atkinson J, Anker S, Braddick O, et al. Visual and visuospatial development in young children with Williams syndrome. Dev Med Child Neurol 2001;43:330–337.
35. Bellugi U, Lichtenberger L, Mills D, et al. Bridging cognition, the brain and molecular genetics: evidence from Williams syndrome. Trends Neurosci 1999;22:197–207.
36. Grady CL, McIntosh AR, Bookstein F, et al. Age-related changes in regional cerebral blood flow during working memory for faces. Neuroimage 1998;8:409–425.
37. Bush G, Luu P, Posner MI. Cognitive and emotional influences in anterior cingulate cortex. Trends Cogn Sci 2000;4:215–222.
38. Tager-Flusberg H, Sullivan K. A componential view of theory of mind: evidence from Williams syndrome. Cognition 2000;76:59–90.
39. Gallagher HL, Frith CD. Functional imaging of 'theory of mind.' Trends Cogn Sci 2003;7:77–83.
40. Druzgal TJ, D'Esposito M. Activity in fusiform face area modulated as a function of working memory load. Brain Res Cogn Brain Res 2001;10: 355–364.
41. Kanwisher N, Stanley D, Harris A. The fusiform face area is selective for faces not animals. Neuroreport 1999;10:183–187.
42. Sergent J, Ohta S, MacDonald B. Functional neuroanatomy of face and object processing. A positron emission tomography study. Brain 1992; 115 Pt 1:15–36.
43. Tsao DY, Freiwald WA, Knutsen TA, et al. Faces and objects in macaque cerebral cortex. Nat Neurosci 2003;6:989–995.
44. Gauthier I, Tarr MJ. Becoming a "Greeble" expert: exploring mechanisms for face recognition. Vision Res 1997;37:1673–1682.
45. Gauthier I, Tarr MJ, Anderson AW, et al. Activation of the middle fusiform "face area" increases with expertise in recognizing novel objects. Nat Neurosci 1999;2:568–573.
46. Wojciulik E, Kanwisher N, Driver J. Covert visual attention modulates face-specific activity in the human fusiform gyrus: fMRI study. J Neurophysiol 1998;79:1574–1578.
47. Grelotti DJ, Gauthier I, Schultz RT. Social interest and the development of cortical face specialization: what autism teaches us about face processing. Dev Psychobiol 2002;40:213–225.
48. Schultz RT, Grelotti DJ, Klin A, et al. The role of the fusiform face area in social cognition: implications for the pathobiology of autism. Philos Trans R Soc Lond B Biol Sci 2003;358(1430):415–427.
49. Maurer D, Le Grand R, Mondloch CJ. The many faces of configural processing. Trends Cogn Sci 2003;6:255–260.
50. Puce A, Allison T, Asgari M, et al. Differential sensitivity of human visual cortex to faces, letterstrings, and textures: a functional magnetic resonance imaging study. J Neurosci 1996;16:5205–5215.
51. Haxby JV, Gobbini MI, Furey ML, et al. Distributed and overlapping representations of faces and objects in ventral temporal cortex. Science 2001;293(5539):2425–2430.
52. Haxby JV, Hoffman EA, Gobbini MI. Human neural systems for face recognition and social communication. Biol Psychiatry 2002;51: 59–67.
53. Tager-Flusberg P-S, Faja S, Joseph RM. People with Williams syndrome process faces holistically. Cognition 2003;89:11–24.
54. Deruelle C, Mancini J, Livet MO, et al. Configural and local processing of faces in children with Williams syndrome. Brain Cogn 1999;41: 276–298.
55. Fink GR, Halligan PW, Marshall JC, et al. Neural mechanisms involved in the processing of global and local aspects of hierarchically organized visual stimuli. Brain 1997;120(Pt 10):1779–1791.
56. Kourtzi Z, Tolias AS, Altmann CF, et al. Integration of local features into global shapes: monkey and human FMRI studies. Neuron 2003;37: 333–346.

Copyright © by AAN Enterprises, Inc. Unauthorized reproduction of this article is prohibited.